Energy 297 (2024) 131286

Contents lists available at ScienceDirect

Energy

journal homepage: www.elsevier.com/locate/energy

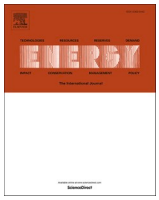

Experimental and computational thermoelectric generator for waste heat recovery for aeronautic application

Qusay Doraghi [a], Alina Żabnieńska-Góra [a], Gabriele Voto [b], Beate Krause [c], Petra Pötschke [c], Ignacio Ezpeleta [d], Cintia Mateo-Mateo [d], Hussam Jouhara [a,e,*]

[a] Heat Pipe and Thermal Management Research Group, College of Engineering, Design and Physical Sciences, Brunel University London, UB8 3PH, UK
[b] Sonaca SA, Route Nationale 5, 6041 Gosselies, Belgium
[c] Department of Functional Nanocomposites and Blends, Leibniz-Institut für Polymerforschung Dresden e.V. (IPF), Hohe Str. 6, 01069 Dresden, Germany
[d] AIMEN Technology Centre, Department of Advanced Materials, Polígono Industrial de Cataboi SUR-PPI-2 (Sector 2) Parcela 3, E36418 O Porriño, Spain
[e] Vytautas Magnus University, Studentu Str. 11, LT-53362, Akademija, Kaunas Distr., Lithuania

ARTICLE INFO

Handling Editor: Dr. A. Olabi

Keywords:
Waste heat recovery
Thermoelectric generators (TEGs)
Aviation efficiency
Environmental responsibility
InComEss project
Model validation
Polymer-based TEGs
Energy generation
COMSOL multiphysics
Computational simulation
Sustainability
Aeronautical applications
Heat transfer

ABSTRACT

This study is a comprehensive exploration of a polymer nanocomposite-based Thermoelectric Generator (TEG) developed within the European project InComEss, specifically designed for aeronautical applications. The focus lies on evaluating the TEG's performance under thermal conditions representative of various aircraft flight stages. The TEG module, consisting of four sections with 17 p-n strips each, is constructed from aerospace-grade polycarbonate, exhibiting dimensions of 50 * 1 * 0.3 mm. In the laboratory phase, the TEG's performance is systematically assessed through a series of experiments. Temperature gradients, ranging from −15 °C to 55 °C, emulate conditions experienced during ascending and descending flight stages. The results indicate promising outcomes, showcasing the potential viability of polymer-based TEGs for aeronautical applications. Specifically, temperature gradients of 40–70 °C, representative of atmospheric conditions and wing leading edge skin conditions, are applied across four test trials. The model validation demonstrates creditable agreement between computational outcomes and experimental data. Insights gained from COMSOL Multiphysics simulations includes temperature distribution, electric potential, and flow dynamics. Simulations conducted under varied temperature ranges provide valuable insights into the TEG's performance variability. Key findings include temperature distribution profiles, electric potential outputs under open and closed-circuit conditions, and a detailed flow analysis within a controlled thermal environment. The validated computational model not only enhances understanding of the TEG's behaviour, but also establishes a foundation for optimizing design parameters to enhance thermoelectric efficiency. The error analysis underscores the model's reliability, exhibiting an average error of 5.68 % between computational and experimental results, reinforcing its suitability for scientific investigations of this nature.

1. Introduction

The global quest for sustainable energy solutions has accelerated in recent years as a result of rising energy demands, increasing environmental issues including air pollution and climate change, and limited supplies of traditional fossil fuels. The aerospace industry is at a crossroads of these issues due to its high energy consumption and strict environmental restrictions. A significant amount of the energy input is always dissipated as waste heat throughout the propulsion process. Previously thought of as an inevitable byproduct of energy conversion, waste heat is now seen as a significant unexplored resource [1].

Waste heat recovery has become an essential approach for reducing energy losses and improving overall effectiveness [2] in several industries, including aviation. Industries may turn a resource that was previously misused into a long-lasting and useful asset by using waste heat. This is especially important for aviation applications, wherein the primary goals are improving fuel efficiency, cutting CO_2 emissions, and extending operational capabilities. The aviation sector, which is

* Corresponding author. Heat Pipe and Thermal Management Research Group, College of Engineering, Design and Physical Sciences, Brunel University London, UB8 3PH, UK.
E-mail address: hussam.jouhara@brunel.ac.uk (H. Jouhara).

https://doi.org/10.1016/j.energy.2024.131286
Received 22 November 2023; Received in revised form 19 March 2024; Accepted 11 April 2024
Available online 13 April 2024

frequently criticised for its negative environmental effects, is now given a rare chance to transform its energy landscape and support international sustainability initiatives with cutting-edge technology [3,4].

Hence, in the quest for greater energy efficiency and environmental responsibility, waste heat recovery has become a major focus, especially in aerospace. This sector, defined by cutting-edge technology, increasing energy demands, and global environmental concerns, is at a pivotal moment, where capturing previously wasted thermal energy offers significant benefits [5].

The aviation industry is characterised by a constant need for increased performance, longer flying distances, and lower carbon footprints. In this situation, waste heat provides an untapped resource with the potential to change the industry's energy perspective. Previously, waste heat was considered to be one of the unavoidable energy losses. Aeronautics obtains an opportunity to increase efficiency while simultaneously advancing the general objective of more environmentally friendly and sustainable flying practises by collecting and turning waste heat into productive power streams [6].

One of the key challenges in aeronautical engineering lies in the delicate balance between power generation and weight considerations [7]. Conventional heat dissipation techniques, such passive cooling systems, not only take up valuable interior space but also contribute to the aircraft's weight. Thermoelectric generators (TEGs), for example, are waste heat recovery devices that circumvent beyond these problems. TEGs provide a sophisticated solution that harmonises with the strict weight restrictions ingrained in aircraft engineering due to their lightweight and compact structure [8].

Additionally, the dynamic nature of flight, which includes a range of temperature gradients and operating phases, emphasises the requirement for a flexible energy recovery strategy. In this dynamic environment, waste heat recovery systems, such as TEGs, flourish and provide a special capability to capture energy under various circumstances. Waste heat recovery systems are ready to optimise energy conversion throughout the course of a flight.

At the nexus of waste heat recovery and aviation applications, thermoelectric generators have emerged as a game-changing option [9]. These devices use the Seebeck phenomenon to convert temperature gradients directly into electrical power, offering a simple and effective way to capture waste heat [10]. TEGs provide significant benefits for aeronautic applications, including:

- Compact Size Factor: TEGs are naturally lightweight and compact, which makes them suitable for integration on an aeroplane [11].
- Decentralized Energy Generation: TEGs enable decentralized energy generation, which lessens dependency on conventional centralised power sources and promotes self-sufficiency in terms of powering onboard systems [12].
- Sustainable Operations: By reusing waste heat, TEGs help the industry achieve its sustainability goals by using less fuel and emitting fewer pollutants [13].
- Operational Flexibility: TEGs can function in a range of temperature gradients, making it possible to effectively collect energy throughout various flight phases, including take-off, cruise, and landing.
- Improved dependability: TEGs' inherent design simplicity translates to improved dependability and fewer maintenance needs, which are crucial for aviation applications where downtime must be kept to a minimum [14].
- TEGs may have the potential to be used to power auxiliary systems, avionics, and even sophisticated sensor networks in addition to propulsion, ushering in a new age of self-sufficient operations [15]. This decentralized energy production, along with the potential for lower fuel use and emissions, paves the way for a concept change in the management of aviation energy.

The use of waste heat recovery technology, notably TEGs, has the potential to significantly alter how energy is managed in the aviation industry. These creative ideas tackle the problems of energy efficiency, environmental impact, and operational adaptability by transforming waste heat into a useable source of energy. For the advancement of fully independent sensor systems or wireless systems within the aviation industry, the utilization of decentralized generation of electrical energy from the surroundings is a crucial factor. This approach facilitates on-site system functionality, enhancing adaptability and allowing convenient system setup devoid of extensive wiring efforts [16]. Moreover, it presents a low-maintenance alternative for sustaining the continuous operation of powered devices. The implementation of energy harvesting could potentially yield economic benefits for both manufacturers and airline companies operating within the aviation sector [17].

As a result, there is potential for cost savings in production, as expenditures on aircraft modification and cabling could be reduced. Furthermore, in comparison to systems reliant solely on wired data transmission, there are opportunities for weight reduction in the context of self-sufficient wireless sensor networks [18]. These weight reductions consequently contribute to decrease operational costs and fuel consumption with the subsequent reduction of CO_2 emissions. Integrating sensor networks into aircraft will enable the monitoring of essential parameters through IoT integration, ultimately leading to reduced maintenance costs. The superiority of wireless and autonomous solutions in terms of weight has been demonstrated. Thus, it has been established that energy harvesting technology plays a pivotal role in enabling wireless sensor networks on airplanes [19].

The InComEss project develops a novel environmentally friendly and economically viable approach for high-efficiency energy harvesting by integrating new intelligent advanced polymer-based composite materials and structures into a single/multi-source concept to harvest electrical energy from mechanical energy and/or waste heat ambient sources [20]. Moreover, the design of the InComEss TEG is a planar one with an in-plane heat transfer to accommodate the wing geometry. Usually, TEGs are based on a 3D solid design with a through-thickness heat transfer. This planar geometry of the TEG is a feature which is only possible by using the newly developed flexible polymer-based TE materials. This paper focuses on the evaluation and validation of the InComEss TEG specifically designed for aeronautical use cases.

While numerous investigations have explored the effectiveness of various thermoelectric systems, this study distinguishes itself by introducing novel material and design considerations tailored for aeronautical applications. In particular, the Thermoelectric Generator (TEG) developed for this research utilizes aerospace-grade polycarbonate, representing a significant advancement in thermoelectric material selection for aeronautical applications. This TEG module is designed with a specific focus on meeting the demanding requirements of aviation use, featuring a unique construction comprising four sections, each containing 17 p-n strips. Notably, the dimensions of these TEG sections, 50 * 1 * 0.3 mm, have been optimized to ensure seamless integration into aircraft components. By evaluating the TEG's performance under thermal conditions representative of various aircraft flight stages, this study offers valuable insights into its feasibility and potential benefits for aviation applications. Furthermore, the research employs a comprehensive approach combining experimental and computational analyses to thoroughly evaluate the TEG's performance, enhancing the reliability and practicality of the findings.

Overall, the study aims to evaluate and validate a novel TEG specifically designed for aeronautical use cases. It encompasses three main aspects: the manufacturing process, experimental evaluation, and numerical assessment of the TEG's performance. The manufacturing process section outlines the unique considerations involved in producing a TEG suitable for aeronautical applications, emphasizing material selection and design optimization. In the experimental evaluation section, comprehensive test results conducted under various temperature differentials are presented, providing valuable insights into the TEG's performance in real-world conditions. Additionally, the numerical assessment section employs advanced computational models to analyse

the TEG's behaviour and validate experimental findings, offering a deeper understanding of the underlying physical phenomena. By integrating these approaches, the study aims to provide a holistic analysis of the TEG's performance and its suitability for aeronautical applications.

2. TEG configurations for the aeronautic use case

2.1. Temperature range

The aeronautic use case defined in this paper is determined by the temperature limits of the wing of the aircraft during service. The envisaged thermal conditions are representative of an aircraft going through clouds during the ascending and descending flight stages, with potential ice accretion around the wing leading edge. The resulting temperature difference between the aerodynamic surface (heated on demand to avoid ice build-up) and the outside environment (usually at temperature below the freezing level) is more relevant along the chordwise direction and such to be exploited to activate the TEG (located within the wing leading edge). Fig. 1(a) shows a wing leading edge cross-section profile with a coloured map indicating the expected temperature variations along the wing surface. The greatest temperature difference is attained on the nose tip in correspondence of the anti-icing protection system, which is continuously operating during the ascending and descending stages. Fig. 1(b) shows the intended location of the TEG patch to grip on the temperature gradient along the skin of the wing leading edge.

For this investigation, a TEG module which was divided into 4 sections, each has 17 p-n pairs, was employed. Each TEG leg has dimensions of 50 *1 * 0.3 mm (leg length x leg width x leg thickness) and it is based on polycarbonate suitable for adoption in aerospace. The definition of a feasible temperature range to be replicated in the test scenario for validating the TEG performance depends on the maximum attainable outside temperature. Past experimental temperature measurements demonstrated that the outside temperature could every so often drop down to −15 °C, while the anti-icing system could operate up to 55 °C. This narrows the temperature range of interest, with a maximum temperature difference of 70 °C. Table 1 indicates the selected temperature gradients within a range of 40–70 °C applied across four test trials to assess the TEG performance. The lower temperature is representative of the atmospheric conditions, whilst the upper temperature is representative of the wing leading edge skin conditions heated up by a heater mat.

Table 1
Selected temperature ranges to assess the TEG performance.

Trial #	Lower temperature (°C)	Upper temperature (°C)	Temperature delta (°C)
1	−15	55	70
2	−10	50	60
3	0	50	50
4	5	45	40

2.2. Materials

Based on polycarbonate (PC, Makrolon 2605 from Covestro), the polymer selected for this application, filled with different carbon nanotube (CNT) types, numerous formulations were developed by melt-mixing on small scale in discontinuous production and their thermoelectric properties were investigated [21] For p type composites, single-walled CNTs of the type Tuball (provided by OCSiAl, Luxembourg) were shown to present the best properties.

For n-type composites, the addition of the switching additive polyethylene glycol (PEG from Sigma-Aldrich, Germany) to SWCNTs was able to induce a change from p-type to n-type behaviour in the PC based composites [22].

Optimized formulations were produced in larger quantities by using a double screw extruder (HAAKE PolyLab QC, Germany) equipped with one feeding point, three heating zones and a final heating die as shown in Fig. 2. The extruder has a counter rotating conical twin-screw with intermeshing screws and a die head section of 2 mm. In the course of upscaling, the formulations were adapted so that the highest possible Seebeck coefficients and high electrical conductivities were achieved.

For the production of the p-type composite, the polymer granulate was first dried at 120 °C during 4 h and then pre-mixed with the selected SWCNTs in a shaker mixer (Turbula T2G from WAB, shown in Fig. 3).

For the production of the n-type PC composite, first the SWCNTs and PEG were pre-mixed in the shaker mixer during 15 min and after this the PC (previously dried) was added to the pre-mix of SWCNT/PEG and mixed again in the Turbula during 30 min, before being introduced in the melt-mixing equipment/extruder [22]. The extrusion temperatures (T1, T2, T3, Td) employed for the compounding of p- and n-type PC composites correspond to 220, 230, 240, 210 °C and 190, 220, 230, 210 °C respectively. The screw speeds were 40 and 30 rpm for p- and n-type PC composites (see Table S4 in ref.[24]). Both types of composites were extruded in the form of filaments and pelletised to be subsequently compressed-moulded into square plates (80 mm × 80 mm x 0.3 mm) by using a hot press (PW40EH, Otto-Paul Weber GmbH, Remshalden, Germany). For shaping, the pellets are placed in a press frame which is placed on a polyimide film to avoid sticking to the heated metal press plates. The cycle used in the hot-press was 2.5 min pre-heating, 1 min pressing with a force of 100 N followed by removal of the sample from the hot press and cooling at 5 °C for 0.5 min. From the compressed-moulded plates, strips of the needed dimensions were cut and assembled in the final device. Images of the extrusion of the PC composite and the bobbins of compounded filaments are shown in Fig. 4. The compression moulding process is also illustrated in Fig. 5.

68 thermoelectric strips electrically grouped in 4 modules (17 strips each module) were placed in a mask and laminated with a bottom polyimide electrode sheet. The layout and pre-manufactured polyimide sheets as well as the cut thermoelectric composite strips are shown in

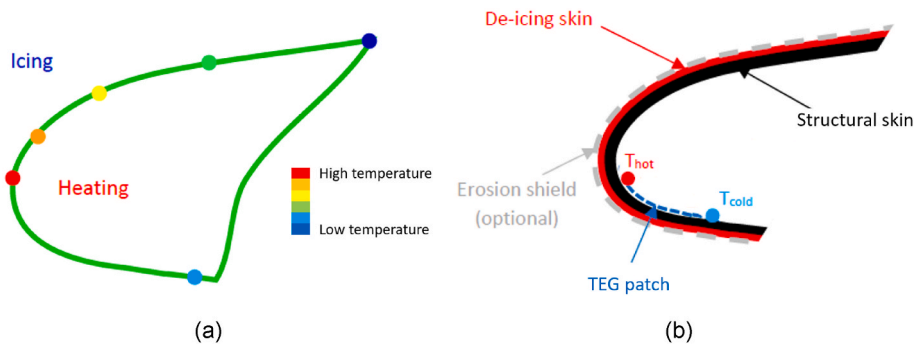

Fig. 1. (a) Temperature distribution along the wing leading edge cross-section and (b) preferred TEG location.

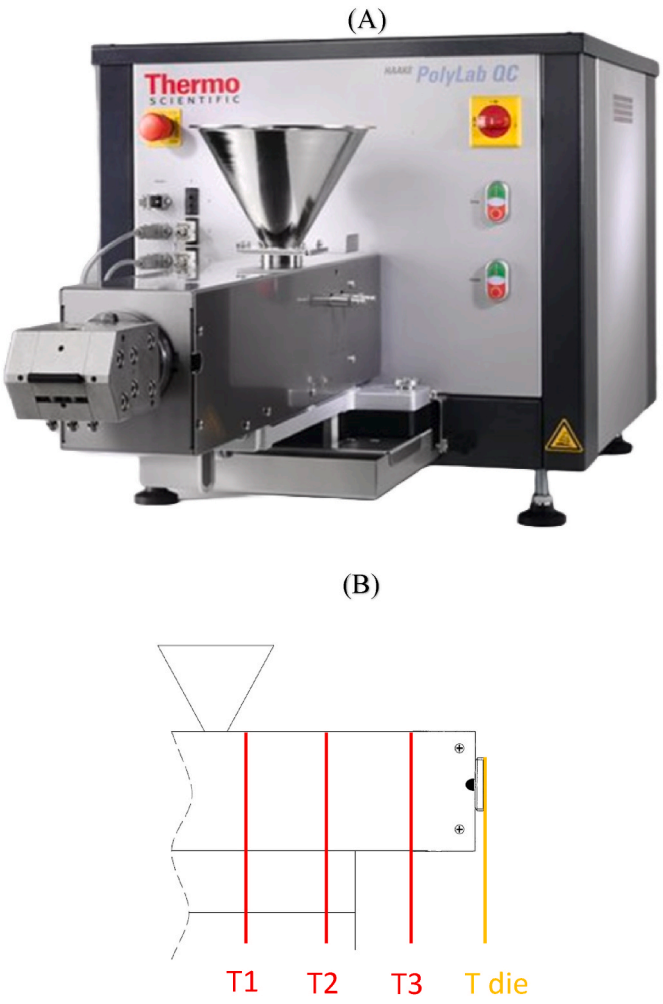

Fig. 2. A) HAAKE PolyLab QC extruder, B) Temperatures zones along the barrel of the extruder.

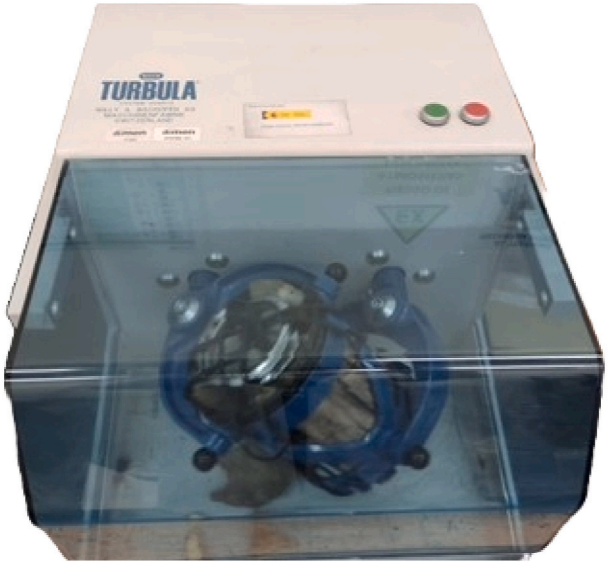

Fig. 3. TURBULA T2G WAB, 3D Shaker mixer [23].

Fig. 6. The P and N strips were placed alternating in the pockets of the mask and after lamination the lab-scaled thermoelectric of the TE generator was ready to be tested. This thermoelectric layer is shown in Fig. 7.

3. TEG measurements in the laboratory

The InComEss TEG performance has been assessed in the defined temperature range, the TEG patch consisting of the combination of p- and n-type PC nanocomposite strips is bonded with a room temperature curing epoxy adhesive on the surface of a representative composite laminate (600 × 340 × 4 mm), whilst the self-adhesive silicone rubber heater mat (250 × 50.8 mm) is bonded on the opposite side across the laminate longitudinal axis. As shown in Fig. 8, the configuration is such that the TEG hot line (i.e., series of white marked squares) must fall in correspondence of the heater mat for generating a local through-the-thickness thermal gradient to activate the patch itself. Fig. 9 shows the laminate as instrumented before testing, with the TEG on the Inner Mould Line (IML) side and the heater mat (HM) on the Outer Mould Line (OML) side.

As shown in Fig. 10(a), the whole assembly is introduced in a thermally insulated climatic chamber with liquid nitrogen blowing in to achieve temperature values compatible with in-flight conditions. The test setup is completed with (a) a cooling unit to ensure the target temperature is within the limit by regulating the nitrogen flow, (b) a power unit to feed the heater mat and an acquisition unit to measure the InComEss TEG generated output voltage through the application of a 1 MΩ input impedance. As shown in Fig. 10(b), the InComEss TEG patch has been covered with insulating material to avoid heat loss between the co-planar hot and cold points of the patch itself. The laminate has also been instrumented with standard T-type thermocouples in critical locations to monitor the temperature distribution during the thermal test.

A series of inspections (i.e., visual/NDT, dimensional, thermographic, and electric) have been completed prior to testing, with evidence of no technical issues both in terms of composite laminate integrity and TEG functioning. As matter of example, Fig. 11 shows the results of a thermographic observation to control the (a) heating capability of the heater mat and (b) the temperature consistency along the heating line on the skin upper side. The temperature distribution is homogeneous in correspondence of the heater mat zone, as evidenced by the thermocouples monitoring the TEG patch and the thermocouple monitoring the heater mat.

Following the achievement of a stable temperature difference (as indicated in Table 2) between the conditioning environment and the InComEss TEG-side laminate skin, the InComEss TEG behaviour has been monitored for at least 5 min in each test trial. Table 2 correlates the experimental lower and upper temperature values to the InComEss TEG output voltage measured during each harvesting test scenario, with values ranging between 67 and 116 mV. The higher the temperature gradient, the higher the voltage; however, these values are deemed insufficient to continuously power up downstream monitoring sensors.

The InComEss TEG element is reactive to the application of an external driving force resulting in the conversion of thermal energy into electricity. However, further development is needed to increase the efficiency and/or the design of polymer-based thermo-electric generator for their integration into aerospace structures for monitoring icing condition risks, whilst guaranteeing a sustainable operation.

4. Computational analysis

4.1. COMSOL multiphysics

In this investigation, the capabilities of COMSOL Multiphysics to model, simulate, and unravel the intricate physical processes within the TEG was leveraged. The selection of COMSOL Multiphysics is underpinned by its robust suite of tools tailored for multifaceted simulations,

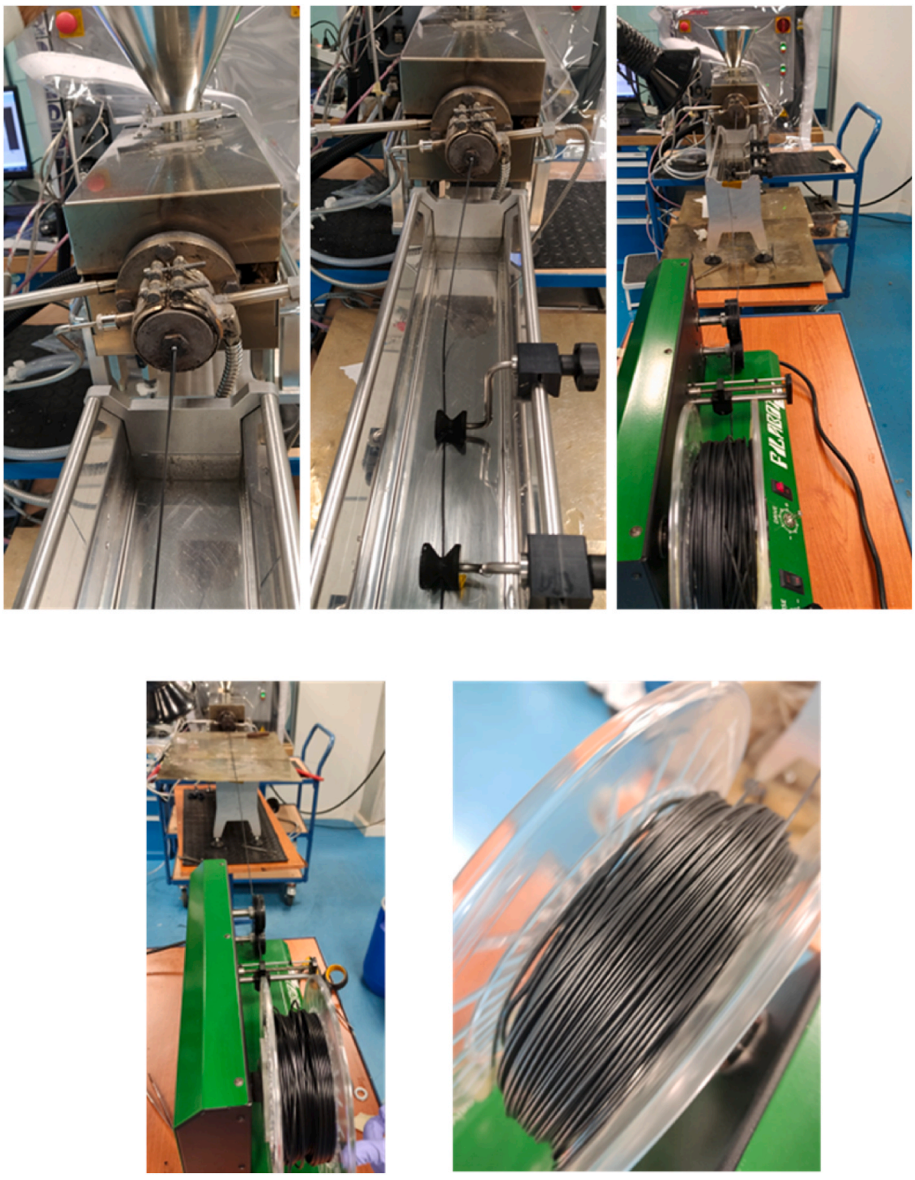

Fig. 4. PC composite extrusion and filament bobbins.

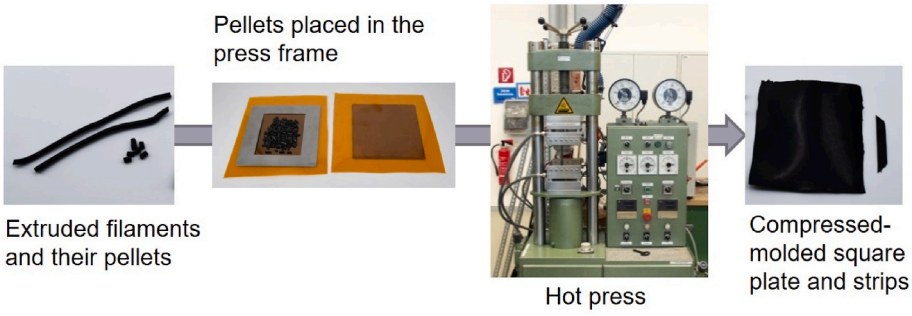

Fig. 5. Schematic process for producing the strips from the extruded filaments by means of compression moulding.

offering a versatile platform that extends beyond generic applications [25]. The following are the reasons why COMSOL Multiphysics was used for this investigation:

- Emphasizing the interplay of phenomena within the TEG system, this research utilised COMSOL, which excels in accommodating multiple coupled physics. This is deemed necessary for an accurate representation of real-world systems [26]. Specifically, this analysis integrated Heat Transfer in Solids, Electric Current, Electric Circuit, and Laminar Flow physics, reflecting the intricate coupling inherent in the TEG's operating environment.

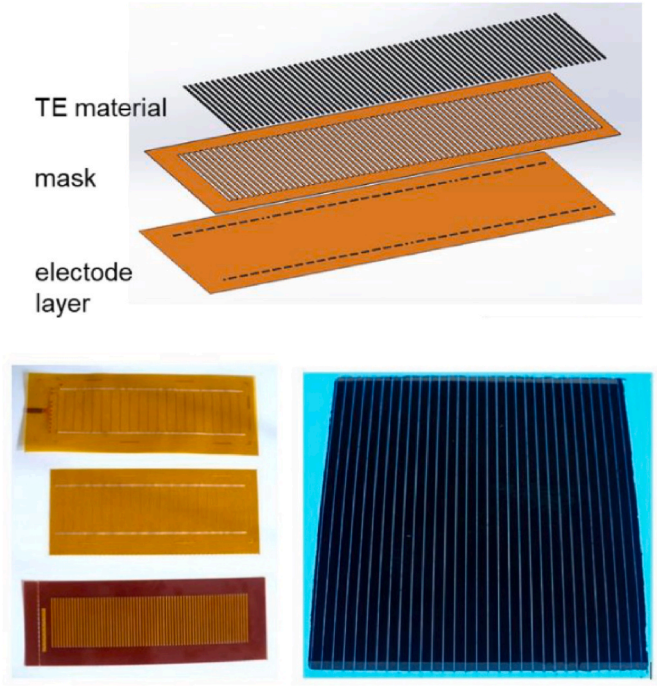

Fig. 6. Schematic design of the generator and generator electrode foils and thermoelectric strips.

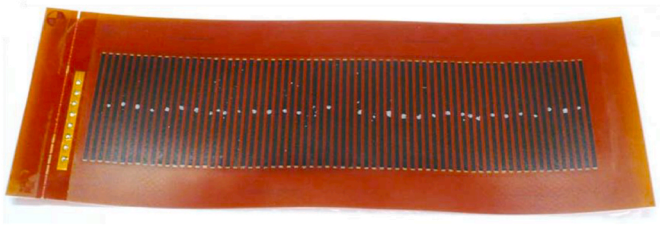

Fig. 7. Thermoelectric layer of the generator.

- Versatility: COMSOL is a valuable tool for many sectors and research disciplines since it can be applied to a wide range of applications, including electrical, mechanical, chemical, and thermal engineering [27].
- Customization: The flexibility of COMSOL is harnessed to tailor simulations specifically for the complex challenges posed by the TEG. The graphical user interface (GUI) facilitates a personalized approach, allowing us to configure simulations that encapsulate the intricacies of TEG behaviour. The ability to employ MATLAB or Python further enhances customization, addressing the unique challenges presented by the TEG structure and materials [28].
- Accuracy: COMSOL's deployment of advanced numerical techniques is paramount in our pursuit of accurate simulations. By effectively handling nonlinear, time-dependent, and coupled physics issues, COMSOL ensures dependable results that capture the dynamic behaviour of the TEG. This commitment to accuracy is essential for deriving meaningful insights into the TEG's performance across varying conditions.
- Visualization: Visualization tools within COMSOL empower researchers to intuitively understand and interpret simulation results. Graphical representation in 2D and 3D, animations, and other visualization techniques facilitate a comprehensive analysis of the TEG's thermal and electrical behaviour. This visual feedback enriches the understanding and aids in drawing meaningful conclusions from the simulations [29].
- Design Optimization: COMSOL may be used for optimization studies to determine the optimal design parameters for a particular situation. This can result in better product designs as well as cost reductions in engineering applications [30].
- Simulation-Based Decision-Making: COMSOL enables researchers to conduct virtual experiments, eliminating the requirement for actual prototypes and experiments. This may save a lot of time and money on product development and research efforts [31].

Overall, the selection of COMSOL Multiphysics is driven by a thorough consideration of the complex physics inherent in the TEG system. By tailoring simulations to encompass these physics, it is aimed to extract valuable insights into the TEG's performance and contribute to the advancement of thermoelectric technology for aeronautical applications.

4.2. *Boundary conditions, meshing and model development*

Based on the information available from the manufacturer, four TEG modules, each containing 17 legs of p-n type, were designed. The dimension of each P–N strip is 50 × 1 × 0.3 mm (leg length × leg width × leg thickness), which is the same as the manufactured TEG; also, each pair is connected through a copper block for electrical continuity as indicated in Fig. 12.

The properties of the material used in the simulation are indicated in Table 3. Properties such as Seebeck coefficient, electrical and thermal conductivity are temperature dependant, however, in this simulation, constant values were implemented.

A variety of numerical approaches are used within the context of COMSOL Multiphysics®, each of which relies on the principle of a Mesh to discretize the modelling space. This Mesh serves two functions in the simulation process. It serves as an approximation of the computer-Aided Design (CAD) geometry first and foremost, offering a structured representation of the physical domain under consideration. Second, it defines discrete points or nodes scattered over the geographic domain from which the approximate solution to the given issue is determined.

Given that mesh refinement is the foundation of numerical precision, its significance becomes clear. The numerical solution eventually converges towards a more accurate representation of the real solution to the boundary value problem being addressed by progressively improving the quality of this Mesh. In fact, the Mesh refinement process makes it possible to reduce mistakes and enhance the alignment between the results of simulations and physical reality, making it a crucial step toward COMSOL Multiphysics® simulations that are accurate and resilient

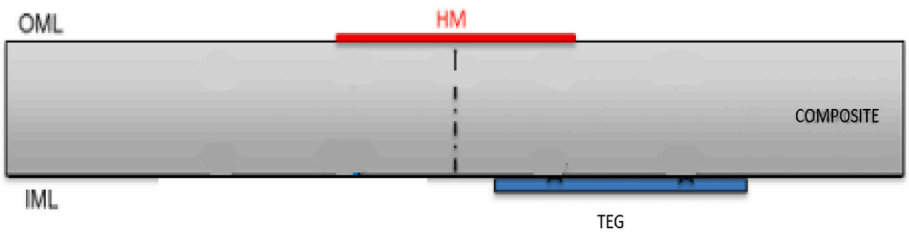

Fig. 8. Schematic of the composite laminate with InComEss TEG and heater mat integration.

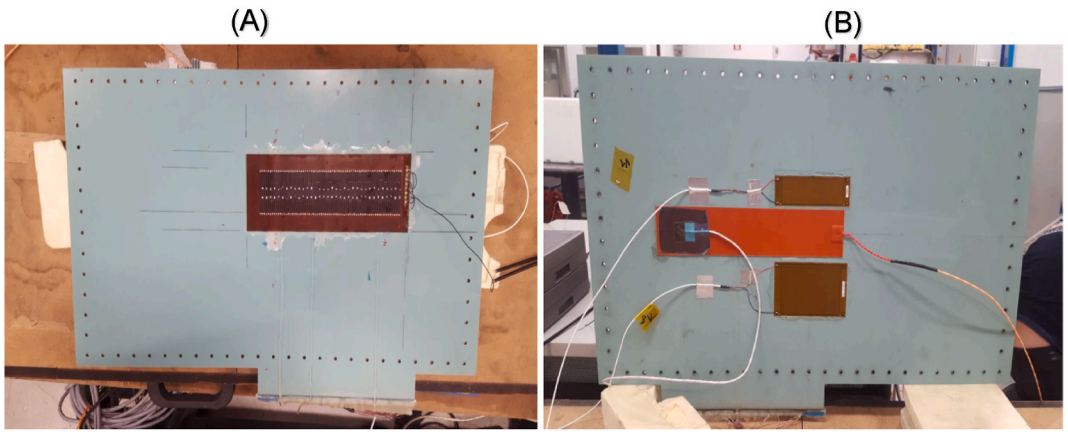

Fig. 9. Instrumented composite laminate for InComEss TEG performance assessment: (a) patch and (b) heater mat side.

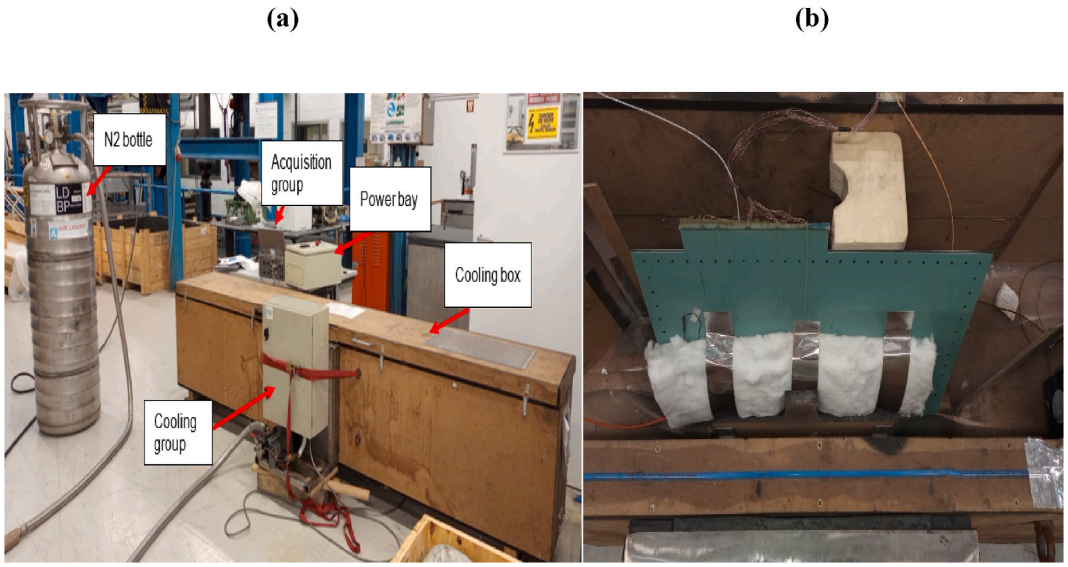

Fig. 10. Test setup configuration: (a) general view and (b) detail on the test demo assembly.

[32]. Table 4 indicated the details of the mesh used for this simulation.

Fig. 13 shows the meshed TEG model which has been simulated for this investigation. In order to fully duplicate the TEG in real life, the TEG was positioned in rectangular shape box as indicated in Fig. 13.

Following the design and meshing of the Thermoelectric Generator module, the next phases required defining the material characteristics, comprehending the underlying processes, and determining the module's boundary conditions. In addition to these preparations, the simulation used two particular COMSOL modules, particularly 'Heat Transfer in Solids' and 'Electric Currents'. These modules were critical components of the simulation framework, allowing for a thorough examination of heat transfer and electrical current flow within the TEG module. By combining these specialised modules, it is possible to obtain a more precise and thorough simulation of the TEG's performance and behaviour, contributing to a better knowledge of its functioning and efficiency. These two physics were introduced comprehensively in previous papers by the authors [9,33].

However, within 'Heat Transfer in Solids' interface, 'Fluid' node was added. This node employs Equation (1) of the heat equation to model heat transfer in fluids:

$$\rho C_p \frac{\partial T}{\partial t} + \rho C_p u.\nabla T + \nabla.q = Q \quad (1)$$

$$q = -k\nabla T$$

Where:

ρ: Fluid density $\left(\frac{kg}{m^3}\right)$.

C_p: fluid heat capacity at constant pressure $\left(\frac{J}{kg.K}\right)$.

k = fluid thermal conductivity $\left(\frac{W}{m.K}\right)$.

u: fluid velocity field, either an analytic expression or a velocity field from a Fluid Flow interface $\left(\frac{m}{s}\right)$.

Q: heat source (or heat sink) $\left(\frac{W}{m^3}\right)$.

Moreover, for this specific simulation, in addition to 'Heat Transfer in Solids' and 'Electric Currents' interfaces, 'Laminar Flow' interface physics was added. The Laminar Flow interface is used to compute the velocity and pressure fields for the flow of a single-phase fluid in the laminar flow regime, this interface has capabilities for handling incompressible, weakly compressible, and low Mach number compressible flows, which includes non-Newtonian fluids. It is also used to solve both the Navier–Stokes equations governing momentum and the continuity equation for conserving mass.

The Laminar Flow interface is applicable to both stationery and time-dependent analyses, with a preference for time-dependent studies when dealing with high-Reynolds number flows, as these tend to exhibit unsteadiness.

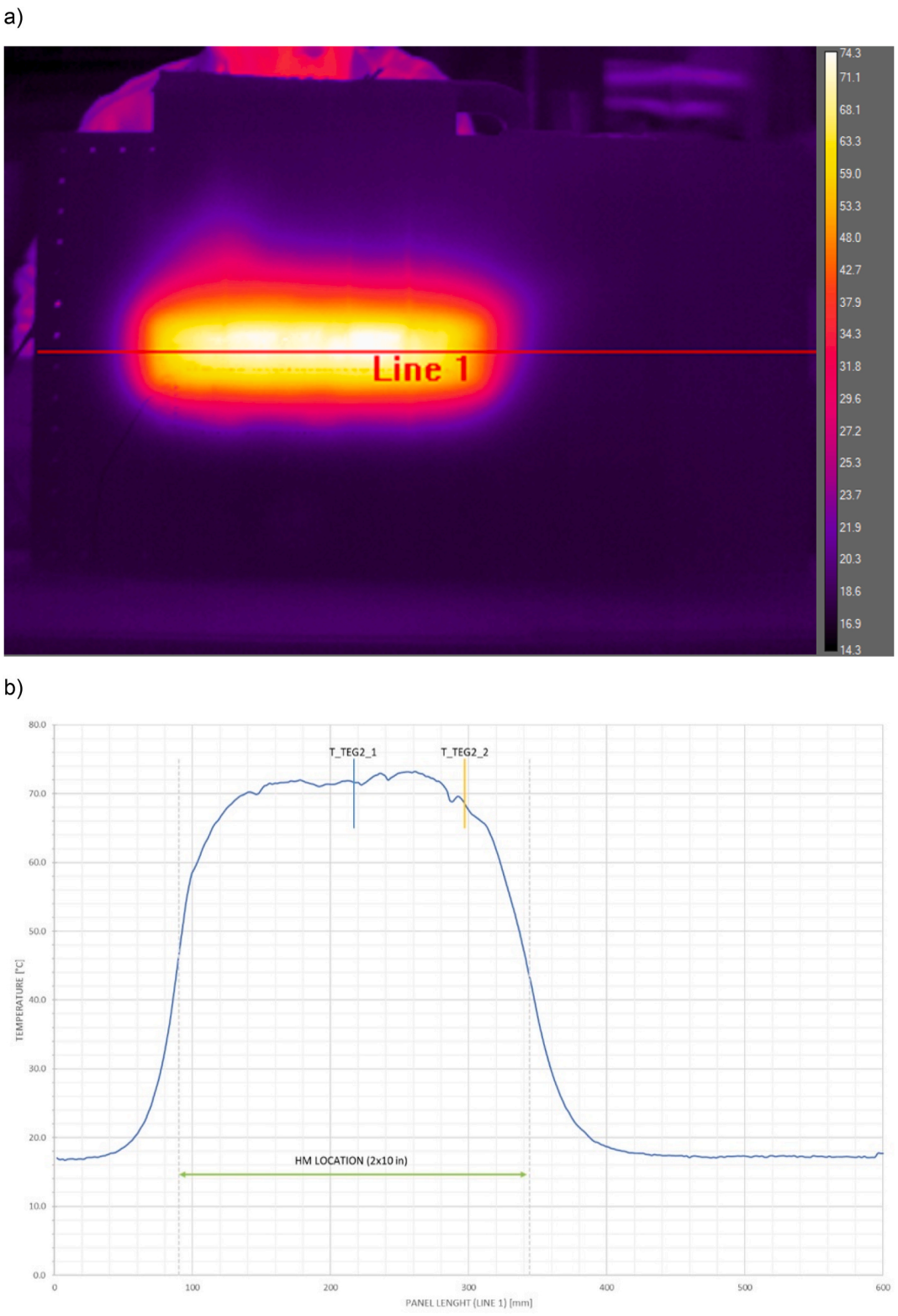

Fig. 11. Thermographic inspection: (a) thermal scan and (b) temperature distribution profile.

By adding the Laminar Flow interface, default nodes such as Fluid Properties, Wall (with a No slip boundary condition as the default), and Initial Values are automatically included, moreover, nodes such as Inlet, Outlet, and Symmetry were also added. Inlet conditions are applied for domains with a net inward flow, and it is recommended to also consider Outlet conditions to ensure problem stability. Outlet conditions are applied to domains with a net outward flow. Symmetry conditions are implemented in cases of geometric and expected solution mirror. When using this node in a model its size could be reduced by one-half or more, making this an efficient tool for solving large problems [34]. It must be mentioned that Air is selected as the working fluid due to its relevance in aeronautical applications and its direct impact on TEG performance. The choice of air aligns with conditions encountered during various flight stages, making this analysis applicable to practical aeronautical

Table 2
InComEss TEG measured output voltages.

Trial #	Lower temperature (°C)	Upper temperature (°C)	Temperature delta (°C)	Output voltage (mV)
1	−14	63	77	116
2	−10	50	60	90
3	0	50	50	85
4	1	41	40	67

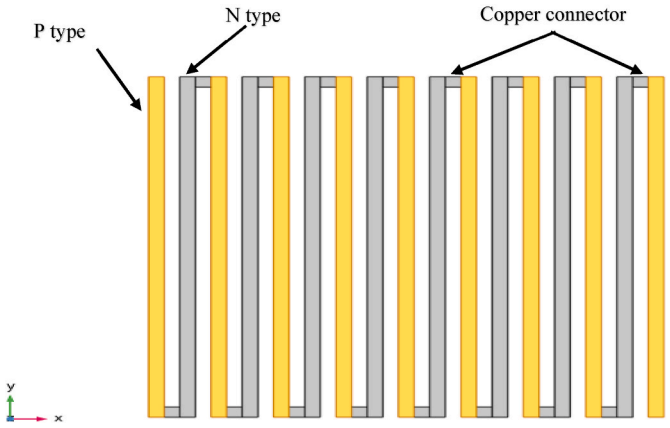

Fig. 12. Material used for the TEG.

Table 3
Material properties used for simulation.

PC - P type			
Property	Variable	Value	Unit
Heat capacity at constant pressure	Cp	1.54	J/(g·K)
Density	rho	930.0	kg/m^3
Seebeck coefficient	S_iso; Sii = S_iso, Sij = 0	36.80	μV/K
Electrical conductivity	sigma_iso; sigmaii = sigma_iso, sigmaij = 0	0.17	S/cm
Thermal conductivity	k_iso; kii = k_iso, kij = 0	0.47	W/(m·K)
Relative permittivity	epsilonr_iso; epsilonrii = epsilonr_iso, epsilonrij = 0	3.0	1.0
PC - N type			
Property	Variable	Value	Unit
Heat capacity at constant pressure	Cp	1.65	J/(g·K)
Density	rho	970.0	kg/m^3
Seebeck coefficient	S_iso; Sii = S_iso, Sij = 0	−56.60	μV/K
Electrical conductivity	sigma_iso; sigmaii = sigma_iso, sigmaij = 0	0.24	S/m
Thermal conductivity	k_iso; kii = k_iso, kij = 0	0.48	W/(m·K)
Relative permittivity	epsilonr_iso; epsilonrii = epsilonr_iso, epsilonrij = 0	3.0	1.0

scenarios.

Moreover, the integration of the 'Electrical Circuit' interface in the simulation framework played a pivotal role in the analysis of currents and voltages within the TEG closed electric circuits. This versatile interface facilitated the modelling of various electrical components, encompassing voltage and current sources, resistors, capacitors, inductors, and semiconductor devices. Notably, the Electrical Circuit interface allowed for seamless incorporation of connections to distributed field models, enabling a comprehensive assessment of circuit behaviour.

Upon the addition of the 'Electrical Circuit' interface, a default 'Ground Node' feature was automatically introduced. This feature is

Table 4
Mesh details.

Mesh type	Quantity
Tetrahedra	4882256
triangles	466477
edge elements	28624
vertex elements	1462
Domain element statics	
number of elements	4882256
minimum element quality	0.002321
average element quality	0.5592
element volume ratio	4.15E-08
Mesh volume	0.025 m^3

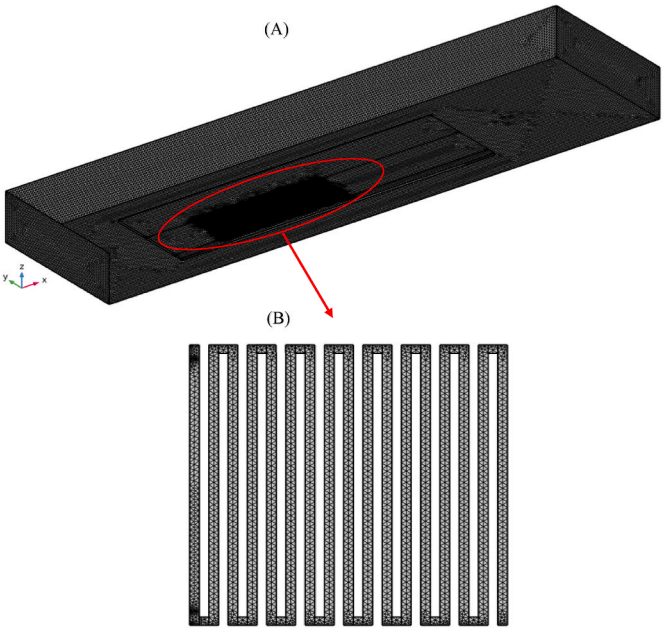

Fig. 13. Meshed model. A) The whole mesh B) Meshed TEG.

associated with node zero within the electrical circuit, serving as a reference point for potential differences and grounding considerations. In addition to the Ground Node, another essential feature which was added within the interface is the 'Resistor'. This feature facilitated the straightforward connection of resistors between two nodes within the electrical circuit, enabling precise control and analysis of resistance properties within the circuitry.

The utilization of the Electrical Circuit interface enables to construct and analyse closed circuit configurations, contributing to a deeper understanding of the electrical characteristics of the TEG module under varying conditions. This interface served as a cornerstone for the electrical analysis and played a crucial role in the interpretation of the simulation results [35].

These thorough boundary conditions, tailored to the specifics of the TEG module and its operational environment, paved the way for a comprehensive simulation. The interplay between thermal, electrical, and fluid dynamics aspects was intricately captured, ensuring that the computational model accurately reflected the real-world behaviour of the polymer nanocomposite-based Thermoelectric Generator under varying conditions. The ensuing sections delve into the results and discussions derived from this robust numerical framework.

4.3. Result and discussion

After setting the boundary conditions and finalising the meshing process, the model was subjected to simulation. This simulation was

conducted in two distinct phases. In the initial phase, the primary focus was on investigating the thermal and electrical performance of the Thermoelectric Generator (TEG), with no consideration for the surrounding environment.

Subsequently, to perform a finite element analysis encompassing the TEG and its immediate surroundings, the TEG setup was placed within a rectangular enclosure. In this setup, a fluid (air) was directed from one end (inlet) to the other end (outlet) of the enclosure. Notably, the ambient air's temperature was set to match that of the heat sink, which was at −15 °C.

4.3.1. Temperature distribution

In this simulation, the baseline conditions were initially established by setting the cold junction temperature to −15 °C and the hot junction temperature to 66 °C. However, to ensure that the simulation closely mirrored the real-world experimental conditions (which were conducted across a spectrum of temperatures), iterative simulations were conducted within specific temperature ranges. These temperature ranges were thoughtfully categorised into four distinct sets to comprehensively capture the experimental scope.

a) -15 °C–66 °C
b) -10 °C–50 °C
c) 0 °C–5 °C
d) 1 °C–41 °C

The results corresponding to each of these temperature ranges will be presented in the Results section of this paper. Fig. 14-A represents the temperature distribution for the TEG at temperature range of −15 °C–55 °C, while Fig. 14-B shows the temperature distribution in the TEG module and its surrounding environment.

4.3.2. Electric potential

The Thermoelectric Generator module employed in this study was constructed as a composite assembly, consisting of four distinct segments. Each of these segments, in turn, incorporated 17 legs of p-n type. Consequently, during the simulation process, it became essential to monitor and record the electrical potential of each individual section.

To facilitate this measurement, all four sections were strategically interconnected in a series configuration. This arrangement allowed for the cumulative determination of the overall electric potential of the TEG module by summing the electric potentials of the individual sections. This approach not only enabled precise electrical characterization but also ensured the comprehensive evaluation of the TEG module's performance across the specified experimental conditions. Fig. 15 shows the electrical potential distribution for the TEG at temperature range of −15 °C–55 °C.

To comprehensively analyse the electrical performance of the Thermoelectric Generator, the simulation approach encompassed two distinct scenarios: open circuit and closed-circuit conditions. To achieve this, the essential preliminary step involved the determination of the TEG's internal resistance, which is a critical parameter for subsequent electrical analysis.

The internal resistance calculation served as a foundation for the simulations under open and closed-circuit conditions. In the open circuit configuration, the TEG operated without an external load, allowing to observe its voltage output under no load conditions. Conversely, in the closed-circuit setup, an external load resistance was systematically applied to the TEG module, simulating real-world operating conditions, and providing insights into its electrical behaviour under load.

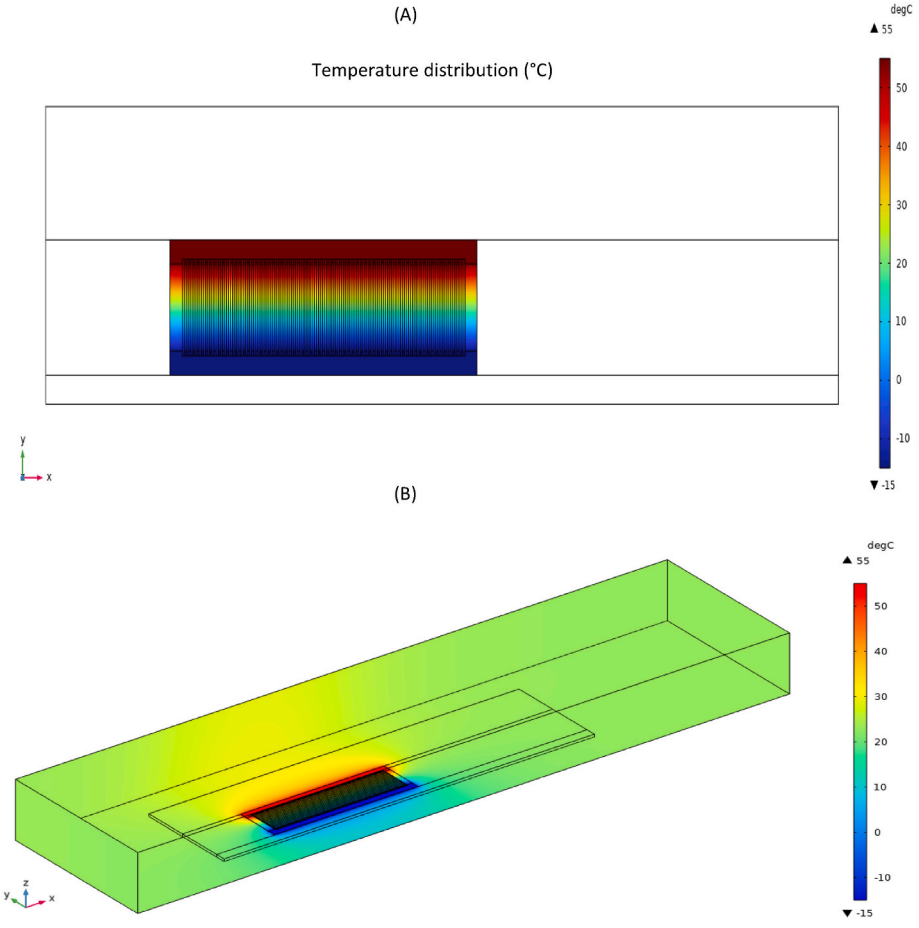

Fig. 14. Temperature distribution for the TEG A) TEG module. B) TEG surrounding environment.

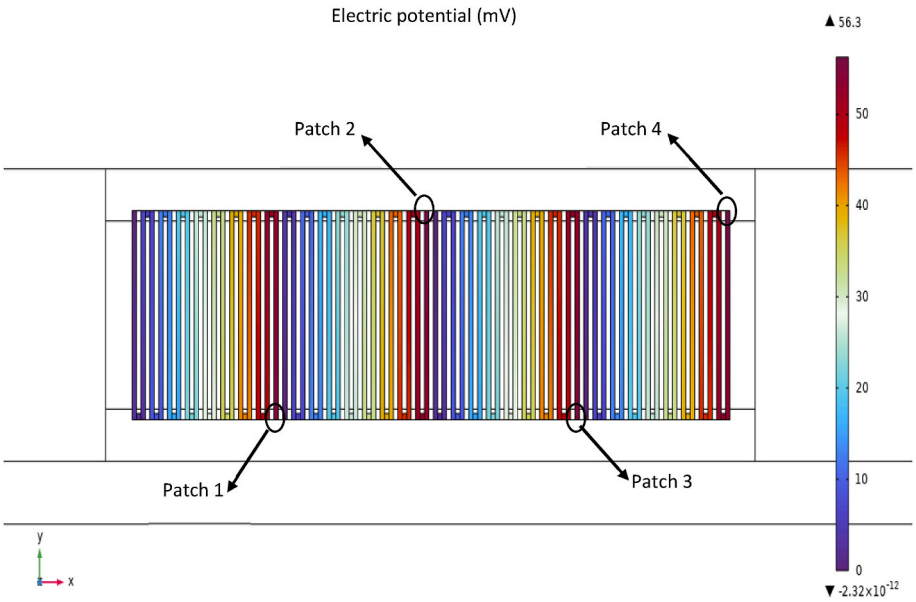

Fig. 15. Electric potential distribution for the patches.

The outcomes of these simulations, under both open and closed-circuit scenarios, are comprehensively documented and presented in Table 5. This table offers a detailed overview of the electrical characteristics of the TEG module, shedding light on its performance across a spectrum of operating conditions, as evident from the data presented in the table, it becomes apparent that a larger temperature differential corresponds to a proportionally greater electrical potential generated by the TEG. It provides essential data that will be discussed and analysed in the subsequent sections of this paper to draw meaningful conclusions and insights.

4.3.3. *Flow analysis*

In order to conduct a finite element analysis on the Hybrid Thermoelectric Generator (TEG) and its surrounding environment, a structured setup was employed. The hybrid TEG was positioned within a rectangular enclosure, and ambient air was introduced into this enclosure through an inlet, flowing towards the opposite end, which served as the outlet.

Maintaining a controlled thermal environment, the ambient air was set to match the standard temperature of 25 °C. This precise temperature control was essential to ensure consistent conditions for the analysis. As depicted in Fig. 16, an observation of the temperature distribution within the enclosure revealed uniformity across most of the space, with notable exceptions occurring around the areas of heat source and heat sink.

For the fluid dynamics aspect of the analysis, a defined velocity profile was imposed at the inlet, where the incoming air exhibited an initial velocity of 5 m/s. Subsequently, the development of the airflow was closely monitored throughout the enclosure. Fig. 16 illustrates the resulting velocity plot for the hybrid TEG and its surroundings.

Table 5
Open circuit and closed circuit Electrical potential values.

Trial	Cold junction (°C)	Hot junction (°C)	Temperature difference (°C)	Electric potential (open circuit) (mV)	Electric potential (closed circuit) (mV)
1	−15	63	77	231.2	122.41
2	−10	50	60	180.2	95
3	0	50	50	149.98	79.6
4	1	41	40	120.04	63.6

This plot reveals a clear trend in the velocity profile. Starting from the inlet, the air exhibited a consistent velocity of 5 m/s, indicating a stable flow. However, as it progressed within the enclosure and encountered the TEG slat, there was a noticeable alteration in its behaviour. Specifically, the velocity experienced a slight increase, reaching 5.6 m/s, before undergoing a subsequent decline.

This change in velocity is indicative of the interaction between the airflow and the hybrid TEG structure, highlighting the localised effects of the TEG on the fluid dynamics within the enclosure. Such insights are invaluable for understanding how the TEG presence influences the thermal and fluid behaviour of the surrounding environment.

4.4. *Model validation*

Model validation plays a crucial role in the assessment of computational models, serving as a fundamental step in ensuring their accuracy and predictive capability. In this context, the COMSOL simulation model was thoroughly compared with experimental data to evaluate its correctness and predictive accuracy, a process depicted in Fig. 17. This comparative analysis was instrumental in assessing the reliability of the computational model and its ability to replicate real-world outcomes.

Fig. 17 offers a visual representation of the results obtained through the COMSOL simulation, alongside with the experimental data. A closer examination of the findings reveals interesting insights. In the initial trials, specifically trials 1 and 2, the simulation results exhibited a slight tendency toward higher output voltage when compared to the corresponding experimental measurements. However, this trend reversed in trials 3 and 4, where the laboratory measurements yielded higher output voltages than those derived from the COMSOL simulations.

It is worth noting that the materials employed in this study, particularly those of PC-based composition, possess properties such as electrical conductivity, thermal conductivity, and the Seebeck coefficient that are known to be temperature-dependent. For the purpose of this simulation, these properties were treated as constant values, a simplification that may have contributed to the observed discrepancies between the computational and experimental results. These deviations underline the importance of considering temperature-dependent material properties in future simulations to achieve even greater accuracy.

To quantify the accuracy of the model, the relative error between the computational and experimental results were calculated for each trial. In trial 1, the error between the two sets of results was a mere 5.5 %,

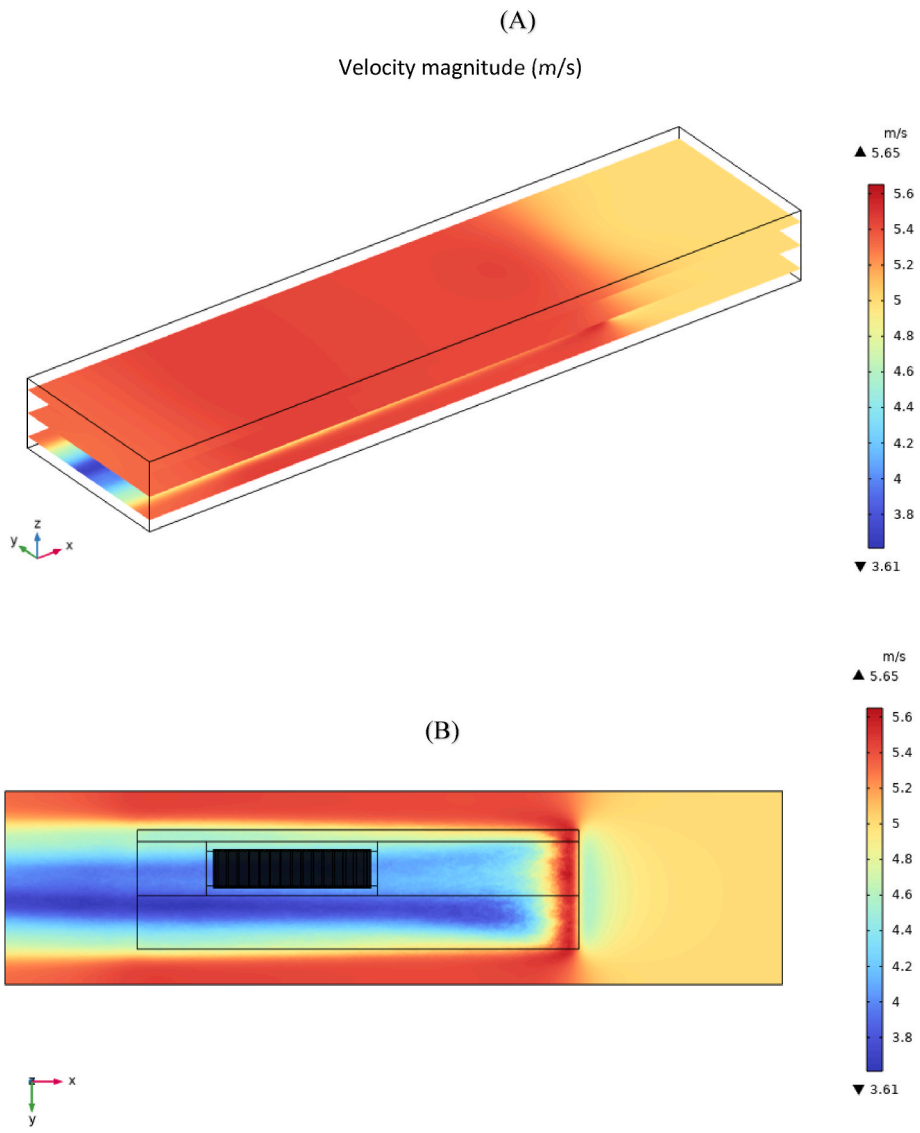

Fig. 16. TEG COMSOL model – Velocity magnitude A) Top overview with temperature B) Bottom view.

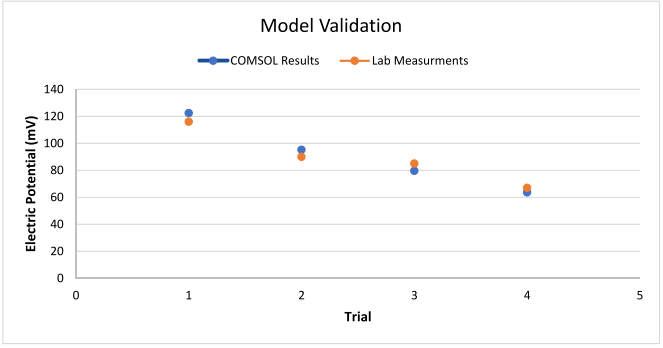

Fig. 17. InComEss TEG output voltages, computational analysis vs. the experimental results.

showcasing the model's reliability. A similar level of precision was maintained in trial 2, with an error of 5.8 %. In trial 3, the error margin slightly increased to 6.3 %, still within an acceptable range of deviation. Finally, for trial 4, the error was 5.1 %, indicating consistent agreement between the model and experimental data.

Despite these variations, the overall consensus drawn from this comparative analysis suggests that the computational model aligns favourably with the experimental observations. Consequently, the computational model can be considered validated, indicating its capability to emulate real-world scenarios with commendable reliability.

5. Conclusion

In this paper, the effectiveness of a polymer nanocomposite-based Thermoelectric Generator, developed as part of the EU project InComEss, was comprehensively evaluated within the context of a typical composite laminate in a controlled temperature environment. To create a thermal gradient for TEG operation, the TEG patch was strategically bonded to the laminate, while a heating pad was positioned on the opposing side. Throughout a series of test runs, wherein temperature gradients were systematically varied, the temperature distribution across the composite laminate and the corresponding voltage outputs generated by the InComEss TEG were monitored.

The observed output voltages from the InComEss TEG ranged from 67 mV to 116 mV, with the variation primarily contingent on the applied temperature gradient. To affirm the precision and predictive capacity of the experimental results, they were subjected to rigorous comparison with those generated by the COMSOL simulation model. The remarkable

congruence between the simulation outcomes and the empirical measurements of the InComEss TEG output voltages attested to the successful validation of the computational model. Moreover, the finite element analysis, incorporating precise temperature control and fluid dynamics simulations, allows for a comprehensive understanding of the Hybrid TEG's performance characteristics and its impact on the surrounding airflow. These findings provide a foundation for optimizing the TEG's design and operational parameters for enhanced thermoelectric efficiency.

It is worth highlighting that the average error between the computational model's results and the laboratory measurements amounted to a modest 5.68 %, further reinforcing the model's reliability and suitability for scientific investigations of this nature.

It is essential to note that while minor discrepancies existed, these errors underscore the robustness of the computational model and its ability to closely replicate real-world observations. Moreover, these results bolster confidence in the accuracy and predictive capability of the InComEss TEG in composite laminate environments.

In summary, these findings indicate significant progress in the development and evaluation of polymer-based TEGs for aeronautical applications. However, further advancements are needed to augment their efficiency and prepare these polymer-based thermoelectric generators for the task of powering monitoring sensors within aeronautical structures, thereby ensuring sustained long-term performance. This study thus contributes meaningfully to the ongoing evolution of TEG technology in the context of aeronautical applications, underscoring the necessity for persistent innovation and refinement in this domain.

CRediT authorship contribution statement

Qusay Doraghi: Data curation, Conceptualization. **Alina Żabnieńska-Góra:** Formal analysis, Data curation. **Gabriele Voto:** Software. **Beate Krause:** Formal analysis, Data curation. **Petra Pötschke:** Formal analysis, Data curation. **Ignacio Ezpeleta:** Formal analysis, Data curation. **Cintia Mateo-Mateo:** Methodology, Data curation. **Hussam Jouhara:** Writing – original draft, Supervision, Methodology, Investigation, Funding acquisition, Conceptualization.

Declaration of competing interest

We wish to confirm that there are no known conflicts of interest associated with this publication and there has been no financial support for this work that could have influenced its outcome.

We confirm that the manuscript has been read and approved by all named authors and that there are no other persons who satisfied the criteria for authorship but are not listed. We further confirm that the order of authors listed in the manuscript has been approved by all of us.

Data availability

Data will be made available on request.

Acknowledgment

This work has been receiving financial support from the European Union's Horizon 2020 Research and Innovation Programme for project InComEss under Grant Agreement Number 862597.

References

[1] Jouhara H, Khordehgah N, Almahmoud S, Delpech B, Chauhan A, Tassou SA. Waste heat recovery technologies and applications. Therm Sci Eng Prog 2018;6:268–89.
[2] Hamid Elsheikh M, et al. A review on thermoelectric renewable energy: principle parameters that affect their performance. Renew Sustain Energy Rev 2014;30:337–55. https://doi.org/10.1016/j.rser.2013.10.027.
[3] Johnson I, Choate WT, Davidson A. Waste heat recovery. Technology and Opportunities in U.S. Industry; 2008. https://doi.org/10.2172/1218716.
[4] S. Brückner, S. Liu, L. Miró, M. Radspieler, L. F. Cabeza, and E. Lävemann, "Industrial waste heat recovery technologies: an economic analysis of heat transformation technologies", doi: 10.1016/j.apenergy.2015.01.147..
[5] Vesely L, Kapat JS, Bringhenti C, Tomita JT, Stoia MF, Jui K. sCO2 waste heat recovery system in aircraft engine. In: AIAA SCITECH 2022 Forum. American Institute of Aeronautics and Astronautics; 2021. https://doi.org/10.2514/6.2022-1407.
[6] Saadon S. Computational modelling of an Organic Rankine Cycle (ORC) waste heat recovery system for an aircraft engine. MATEC Web Conf. 2018;151. https://doi.org/10.1051/matecconf/201815102001.
[7] Leal Filho W, et al. Global tourism, climate change and energy sustainability: assessing carbon reduction mitigating measures from the aviation industry. Sustain Sci 2023;18(2):983–96. https://doi.org/10.1007/s11625-022-01207-x.
[8] Jouhara H, et al. Thermoelectric generator (TEG) technologies and applications. Int. J. Thermofluids 2021;9:100063. https://doi.org/10.1016/j.ijft.2021.100063.
[9] Doraghi Q, et al. Investigation and computational modelling of variable TEG leg Geometries. ChemEngineering 2021;5(3). https://doi.org/10.3390/chemengineering5030045.
[10] Kuroki T, Kabeya K, Makino K, Kaibe H, Hachiuma H, Fujibayashi A. Waste heat recovery in Steelworks using a thermoelectric generator BT. Proceedings of the 11th European Conference on Thermoelectrics 2014:143–9.
[11] L. P. e Santos and. In: Estudo da aplicação e desenvolvimento de um gerador termoelétrico para cogeração em automóveis; 2020. https://repositorio.ufpb.br/jspui/handle/123456789/19925. [Accessed 29 August 2023].
[12] Fairbanks J. Vehicular thermoelectric applications. 2008.
[13] Gonçalves LM. In: Microssistema termoeléctrico baseado em teluretos de bismuto e antimónio; 2008 [Online]. Available: https://repositorium.sdum.uminho.pt/handle/1822/8171. [Accessed 29 August 2023].
[14] Ando Junior OH, Maran ALO, Henao NC. A review of the development and applications of thermoelectric microgenerators for energy harvesting. Renew Sustain Energy Rev 2018;91:376–93. https://doi.org/10.1016/J.RSER.2018.03.052.
[15] Thielen M, Sigrist L, Magno M, Hierold C, Benini L. Human body heat for powering wearable devices: from thermal energy to application. Energy Convers Manag 2017;131:44–54. https://doi.org/10.1016/J.ENCONMAN.2016.11.005.
[16] Paradiso JA, Starner T. Energy scavenging for mobile and wireless electronics. IEEE Pervasive Comput 2005;4(1):18–27. https://doi.org/10.1109/MPRV.2005.9.
[17] Ziolkowski P, Zabrocki K, Müller E. TEG design for waste heat recovery at an aviation jet engine nozzle. Appl Sci 2018;8(12). https://doi.org/10.3390/app8122637.
[18] Samson D, Otterpohl T, Kluge M, Schmid U, Becker T. Aircraft-specific thermoelectric generator module. J Electron Mater 2010;39(9):2092–5. https://doi.org/10.1007/s11664-009-0997-7.
[19] Dilhac J-M, Monthéard R, Bafleur M, Boitier V, Durand-Estèbe P, Tounsi P. Implementation of thermoelectric generators in airlinersfor powering battery-free wireless sensor networks. J Electron Mater 2014;43(6):2444–51. https://doi.org/10.1007/s11664-014-3150-1.
[20] InComEss." https://www.incomess-project.com/(accessed December. 15, 2022).
[21] Krause B, Barbier C, Kunz K, Pötschke P. Comparative study of singlewalled, multiwalled, and branched carbon nanotubes melt mixed in different thermoplastic matrices. Polymer (Guildf). 2018;159:75–85. https://doi.org/10.1016/J.POLYMER.2018.11.010.
[22] Krause B, Pötschke P. Polyethylene glycol as additive to achieve N-conductive melt-mixed polymer/carbon nanotube composites for thermoelectric application. Nanomaterials 2022;12(21):3812. https://doi.org/10.3390/NANO12213812.
[23] Willy A. Bachofen. TURBULA 2023 [Online]. Available: https://www.wab-group.com/media/2023/04/WAB_Turbula_EN_2023-08.pdf.
[24] Krause B, Imhoff S, Voit B, Pötschke P. Influence of polyvinylpyrrolidone on thermoelectric properties of melt-mixed polymer/carbon nanotube composites. Micromachines Jan. 2023;14(1):181. https://doi.org/10.3390/MI14010181/S1.
[25] Pryor Roger W. Multiphysics modelling using COMSOL. fifth ed. London, UK: David Pallai; 2011.
[26] Jafari A, Vahab M, Broumand P, Khalili N. An eXtended finite element method implementation in COMSOL multiphysics: thermo-hydro-mechanical modeling of fluid flow in discontinuous porous media. Comput Geotech 2023;159:105458. https://doi.org/10.1016/j.compgeo.2023.105458.
[27] Comsol AB. Introduction to COMSOL multiphysics, vol. 4. Version; 2018. p. 1998–2010.
[28] Gerlich V, Sulovská K, Zálešák M. COMSOL Multiphysics validation as simulation software for heat transfer calculation in buildings: building simulation software validation. Measurement 2013;46(6):2003–12. https://doi.org/10.1016/j.measurement.2013.02.020.
[29] The COMSOL Product Suite," https://www.comsol.com/products.
[30] Vakkada Ramachandran A, Zorzano M-P, Martín-Torres J. Numerical heat transfer study of a space environmental testing facility using COMSOL Multiphysics. Therm Sci Eng Prog 2022;29:101205. https://doi.org/10.1016/j.tsep.2022.101205.
[31] Draper A, McKibben N, Estrada D, Deng Z. Multiphysics modeling of printed surface acoustic wave thermometers. Sensors Actuators A Phys 2023;359:114491. https://doi.org/10.1016/j.sna.2023.114491.
[32] Performing a Mesh Refinement Study - Knowledge Base." https://www.comsol.com/support/knowledgebase/1261 (accessed September. 05, 2023).
[33] Doraghi Q, Żabnieńska-Góra A, Norman L, Krause B, Pötschke P, Jouhara H. Experimental and computational analysis of thermoelectric modules based on

melt-mixed polypropylene composites. Therm Sci Eng Prog 2023;39:101693. https://doi.org/10.1016/J.TSEP.2023.101693.
[34] CFD Module User's Guide. www.comsol.com/blogs. [Accessed 5 September 2023].
[35] Comsol. The AC/DC module user's guide. 2020 [Online]. Available: www.comsol.com/blogs. [Accessed 6 September 2023].